

Enhancing superplasticity of engineering ceramics by introducing BN nanotubes

Qing Huang¹, Yoshio Bando¹, Xin Xu², Toshiyuki Nishimura¹, Chunyi Zhi¹, Chengchun Tang¹, Fangfang Xu³, Lian Gao³ and Dmitri Golberg¹

¹ Nanoscale Materials Center, National Institute for Materials Science, 1-1, Namiki, Tsukuba, Ibaraki 305-0044, Japan

² Department of Materials Science and Engineering, University of Science and Technology of China, Hefei 230026, People's Republic of China

³ Shanghai Institute of Ceramics, Chinese Academy of Sciences, Shanghai 200050, People's Republic of China

E-mail: Huang.Qing@nims.go.jp and xuxin@ustc.edu.cn

Received 10 June 2007, in final form 1 October 2007

Published 30 October 2007

Online at stacks.iop.org/Nano/18/485706

Abstract

Introducing carbon nanotubes (CNTs) into polymer or ceramic matrices has been a promising approach to obtain ultra-strong, extra-toughened materials as well as multifunctional composites. Most of the previous work on CNT composites has focused on strengthening and toughening of matrix materials at ambient conditions. However, so far there is a lack of information on the mechanical behavior of these composites at elevated temperature. Recently, single-walled CNTs were found to undergo a superplastic deformation with an appealing 280% elongation at a high temperature (Huang *et al* 2006 *Nature* **439** 281). This discovery implies the high probability for the potential usage of CNTs as reinforcing agents in engineering high-temperature ceramics with improved ductility. Here, for the first time, we demonstrate that a small addition of boron nitride nanotubes (BNNTs) can dramatically enhance the high-temperature superplastic deformation (SPD) of engineering ceramics. More specifically, 0.5 wt% addition of BNNTs leads to an inspiring brittle-to-ductile transition in Al₂O₃ ceramics even at a moderate temperature (1300 °C). For Si₃N₄ ceramics, 0.5 wt% addition of BNNTs could also decrease the true stress by 75% under the same deformation conditions. In contrast, addition of micro-sized or nano-sized BN powders has no or a negative effect on the superplasticity of these ceramics. The underlying SPD-enhancement mechanism is discussed in terms of the inhibition of static and dynamic grain growth of the matrix and the energy-absorption mechanism of BNNTs. The unraveled capability of BNNTs to enhance the SPD behavior will make BNNTs promising components in cost-effective complex ceramics with good comprehensive mechanical properties.

1. Introduction

Introducing carbon nanotubes (CNTs) into polymer or ceramic matrices has been a promising approach to obtain ultra-strong, extra-toughened materials as well as multifunctional composites [1]. However, the use of CNTs to toughen and strengthen materials has been hindered due to their relatively poor oxidation-resistance and tendency to react with other

starting powders such as Si₃N₄, Al₂O₃, etc, which will inevitably cause degradation of CNTs and ceramic mechanical performance because of the cavity appearance. Boron nitride, on the other hand, due to its excellent chemical inertness and oxidation resistance has been widely used in the fabrication of machinable ceramic composites and solid lubricants. Boron nitride nanotubes (BNNTs) have been found to possess a comparable Young's modulus ($E \sim 1.2$ TPa) and thermal

conductivity to those of CNTs [2]. Thus, it is attractive to investigate the mechanical properties of BNNT incorporated composites. Most of the previous work on CNT composites has focused on strengthening and toughening matrix materials at ambient conditions. BNNT-reinforced glass composites have also been reported, those revealed an increased strength and fracture toughness at room temperature [3]. However, so far there has been a lack of information on the mechanical behavior of these composites at elevated temperature [4].

Polycrystalline ceramics have excellent strength, hardness and chemical stability, but their stiffness and brittleness makes it difficult for the fabrication of complicated components at a low cost. This largely limits their broad industrial applications. Since the discovery of superplasticity in Y_2O_3 -stabilized tetragonal ZrO_2 ceramics [5], there have been a few works devoted to superplasticity in varied ceramic materials [6]. Numerous approaches have been developed using a high-strain-rate and low-temperature regime and the composition, microstructure and processing parameters have been optimized [7]. The superplastic deformation (SPD) mechanism in ceramics is still under consideration; the roles of grain size and grain boundary (GB) phase are universally recognized to be crucial for the SPD process. They could be generalized from the following semiempirical relationship: $\dot{\epsilon} = A(\frac{b}{d})^p(\frac{\sigma}{E})^n \exp(-\frac{Q}{k_B T})$, where $\dot{\epsilon}$ is the strain rate, A is a temperature-dependent, GB-diffusion-related coefficient, b is the Burgers vector, d is the grain size, p is the grain-size exponent, σ is stress, E is the Young's modulus, n is the stress exponent, Q is the activation energy for SPD and k_B is the Boltzmann's constant. It can be deduced that reducing the initial grain size d of ceramics and suppressing dynamic grain growth during the deformation process favor the realization of superplasticity. These approaches could be achieved through the incorporation of other phases to inhibit mass diffusion during sintering or deformation processes. For example, Kim and co-workers reported high-strain-rate superplasticity in a nano-sized composite of zirconia, alumina, and spinel with a large tensile elongation of 1050% at a strain rate of 0.4 s^{-1} [8]. One of the disadvantages of this method would be the inevitable sacrifice of the inherent ceramic properties due to the incorporation of a high-volume-ratio second phase (such as reduced overall Young's modulus). On the other hand, the usage of nanocrystalline phases with a high-aspect-ratio, especially one-dimensional nanotubes, is promising and has shown some exciting results in advanced composites [9]. Recently, single-walled CNTs were found to undergo a superplastic deformation with an appealing 280% elongation at a high temperature [10]. This discovery implies the high probability for the potential usage of CNTs as reinforcing agents in engineering high-temperature ceramics with an improved ductility.

Here, for the first time, we demonstrate that a small addition of BNNTs can dramatically enhance a high-temperature superplastic deformation (SPD) of engineering ceramics. More specifically, 0.5 wt% addition of BNNTs leads to an inspiring brittle-to-ductile transition in Al_2O_3 ceramics even at a moderate temperature (1300°C). For Si_3N_4 ceramics, 0.5 wt% addition of BNNTs could also decrease the true stress by 75% under the same deformation conditions. In contrast, addition of micro-sized or nano-sized BN powders has no or negative effect on the superplasticity of these ceramics.

2. Experimental details

As-synthesized BN nanotubes were used without further purification. The ceramic powders were mixed with BN nanotubes wrapped by PVP polymer in ethanol solution. Then the composite powders were filtrated out and calcined at 700°C to burn out the PVP polymer. A spark plasma sintering system (Sumitomo Coal Mining Co. Ltd, Tokyo, Japan), was employed to obtain dense composite ceramics.

Hardness was obtained on an indentation hardness tester (Akashi, AVK-A); Young's moduli were measured using ultrasonic equipment with an oscilloscope (Tektronix TDS 3052B). Deformation of specimens was assessed by uniaxial compression testing, in which compression was applied perpendicular to the direction of SPS. Specimens in this test were 3 mm by 2.5 mm in cross-section and 5 mm in height.

Transmission electron microscopy (JEM-3000F; JEOL) and scanning electronic microscopy (JSM-6700F) were used to observe the microstructures of composites.

3. Results and discussion

Utilized BNNTs had an average diameter of 60 nm and a length over several tens of micrometers [11]. The purity of as-synthesized BNNTs is as high as 97%. Under TEM observation, no obvious catalyst particles were found on the BNNTs. The composite powders were firstly synthesized through mixing commercial alumina powders (particle size $\sim 100 \text{ nm}$) or Si_3N_4 powders (a mixture of amorphous and nano-sized β - Si_3N_4 grains, prepared according to [12]) with BNNTs preliminary sonicated over 30 min in a 1 wt% polyvinylpyrrolidone (PVP) ethanol solution. It is critical to use PVP polymers that make BNNTs evenly dispersive in composite powders and ultimate ceramics. With the aid of PVP wrapping, BNNTs stably suspend in ethanol for at least one week (figure 1(a)). TEM give further evidence that a layer of PVP polymer coats on the sidewall of BNNT (figure 1(b)). The PVP polymer was finally removed through pre-calcining in air at 700°C for 1 h. Spark plasma sintering (SPS) in an Ar atmosphere or N_2 atmosphere was employed to obtain dense polycrystalline ceramics for Al_2O_3 or Si_3N_4 , respectively. The details of the sintering conditions are summarized in table 1.

Fully densified pure Al_2O_3 and BNNT/ Al_2O_3 composites were obtained at 1500°C for 3 min. The microstructure of 0.5 wt% BNNT/ Al_2O_3 composite consisted of equiaxed Al_2O_3 grains and BNNTs embedded at the grain boundaries, as depicted in field-emission transmission electron microscopy (TEM) images (figure 1(c)). A high-resolution TEM image shows that a BNNT well preserves its tubular structure after sintering and is sandwiched between the two Al_2O_3 grains with the respective zone axes of $[2\bar{2}1]$ and $[\bar{4}41]$ (figure 1(d)). The lattice spacing of 0.33 nm is also clearly visible on one side of the BNNT wall, whereas it becomes not well seen on the other side, which is due to the characteristic double-helix structure in as-synthesized BNNTs [13]. No other phases or an amorphous interlayer are visible at the BNNT and Al_2O_3 grain interface due to the ultra-short annealing time and moderate sintering temperature [14]. X-ray diffraction data further confirmed that the products are mainly comprised of BNNTs and Al_2O_3 (figure 2). The average Al_2O_3 grain diameter in a 0.5 wt%

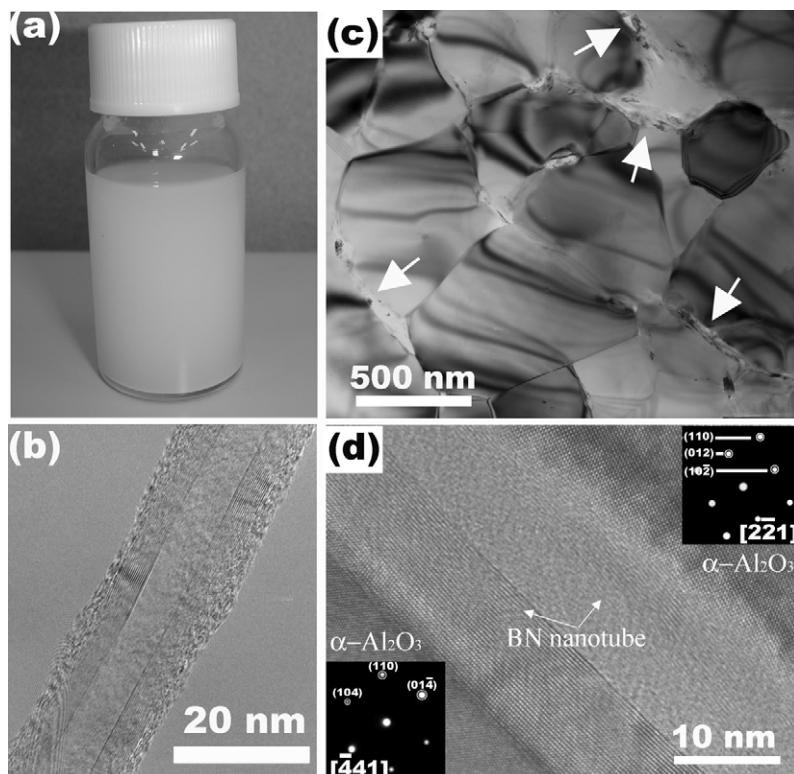


Figure 1. (a) 5 mg BNNTs dispersed in 6 ml ethanol form a stable suspension. (b) TEM image showing single BNNT wrapped by PVP polymer. (c) TEM image of a 0.5 wt% BNNT/Al₂O₃ composite and (d) high resolution TEM image showing a BN nanotube locating at the ceramic grain boundary.

Table 1. Sintering conditions, physical and mechanical properties of products.

Materials	Sintering conditions			Mechanical properties	
	Temperature (°C)	Duration (min)	Relative density (%)	Vickers hardness (GPa)	Young's modulus (GPa)
Al ₂ O ₃	1500	3	100	17.3 ± 0.6	400
0.5 wt% BNNT/Al ₂ O ₃	1500	3	98.2	19.1 ± 0.7	379
2.5 wt% BNNT/Al ₂ O ₃	1500	3	97.1	14.5 ± 0.5	359
Si ₃ N ₄	1600	5	98.5	18.3 ± 0.3	300
5 wt% BN _p /Si ₃ N ₄	1750	5	99.5	11.8 ± 0.8	249
5 wt% BN _n /Si ₃ N ₄	1650	5	98.2	15.1 ± 0.7	243
0.5 wt% BNNT/Si ₃ N ₄	1600	5	97.3	15.5 ± 0.6	273

composite is reduced to 600 nm which is about one fifth of that in a pure Al₂O₃ ceramic (figures 3(a) and (c)). This means that BNNTs could remarkably inhibit the mass diffusion between the matrix grains and suppress the grain growth. This is consistent with the previous studies on CNT filled ceramics with fine-grain microstructures [15].

The 0.5 wt% BNNT/Al₂O₃ composite becomes harder than the BNNT-free Al₂O₃ (table 1), which is due to its strengthened GBs and superfine microstructure according to the Hall–Petch mechanism. Another important parameter, the Young's modulus, decreases in composites even though BNNTs have huge E . There are two major reasons for this deviation from a continuum model which predicts a higher Young's modulus in the composite-filled harder material. Firstly, as the Al₂O₃ grain size decreases, the fraction of triple GB increases. This provides more space to accommodate a strain in the composites. Secondly, since the BNNTs are

confined with stiff ceramic grains and not freely residing as in polymer composites, this waviness configuration results in a remarkable reduction of the effective Young's modulus [16]. In the case of the BNNT/Si₃N₄ composite, a small amount of BNNTs plays a negligible role for the final Si₃N₄ grain size and microstructure (figure 3(e)), but still decreases the relative density and Young's modulus. Even so, the BNNT composites possess a Young's modulus which is more than 90% of that of the starting ceramics.

SPD was performed on a machined 5 × 3 × 2.5 mm³ sample. Compressive force was applied on a 3 × 2.5 mm² sector at a constant crosshead-displacement-rate and released when a shrinkage reached half of the initial height (2.5 mm), as described in detail elsewhere [17]. Obviously, under a constant strain rate of 10⁻⁴ s⁻¹ pure alumina ceramics underwent an elastic deformation at the beginning, but readily cracked when a true strain had reached 0.1 at 1450 °C (figure 4(a)).

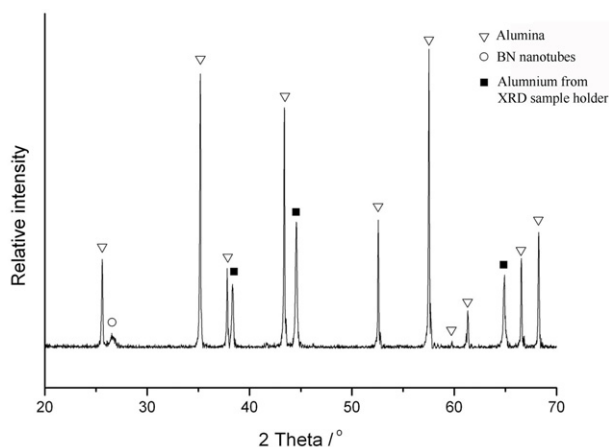


Figure 2. XRD spectrum of a 2.5 wt% BNNT/Al₂O₃ composite.

The fracture surface of the deformed pure alumina sample disclosed that Al₂O₃ grains obeyed dissolution–precipitation rule and dynamically grew to huge rough agglomerates via GB sliding (figure 3(b)). Cavitation was also evidently prevailing. If these cavities are not effectively accommodated through GB diffusion and/or grain dislocation, cavities would be transformed into penetrable cracks and ultimately break

the ceramics. In other words, the accommodation length is proportional to the grain size dynamically mounted in pure Al₂O₃ ceramics, which makes the ceramics brittle and incapable of superplastic deformation. More intriguingly, the deformation feature of Al₂O₃ ceramics is qualitatively changed via addition of BNNTs. The 0.5 wt% BNNT/Al₂O₃ composite shows excellent SPD behavior with a true stress of only 7.5 MPa at 1450 °C (figure 4(a)). Because the strain rate increases during deformation tests due to a decreasing specimen height, the true stress under the initial strain rate is defined as the intersection of two lines extrapolated to the elastic and the plastic strain regions on the stress–strain curves. The true stress at 1400 °C is 14 MPa, which is only one third of the reported value of a 10 vol% ZrO₂/Al₂O₃ composite (about 42 MPa) [18]. Moreover, it is striking to observe that the SPD behavior in 0.5 wt% BNNT/Al₂O₃ composite is maintained even at a temperature as low as 1300 °C which is the lowest deformation temperature reported for alumina ceramics (figure 4(b)) [19]. Assuming the stress exponent n is 2, an activation-energy of 298 ± 63 kJ mol⁻¹ was obtained from plotting of the $\ln \dot{\epsilon} - 1/T$ relationship. This value is far below the reported activation energy (600–800 kJ mol⁻¹) for alumina-based composites whose SPD behaviors were controlled by the diffusion and defect mechanism [20]. It is also worth noting that besides a reduced initial grain size in the

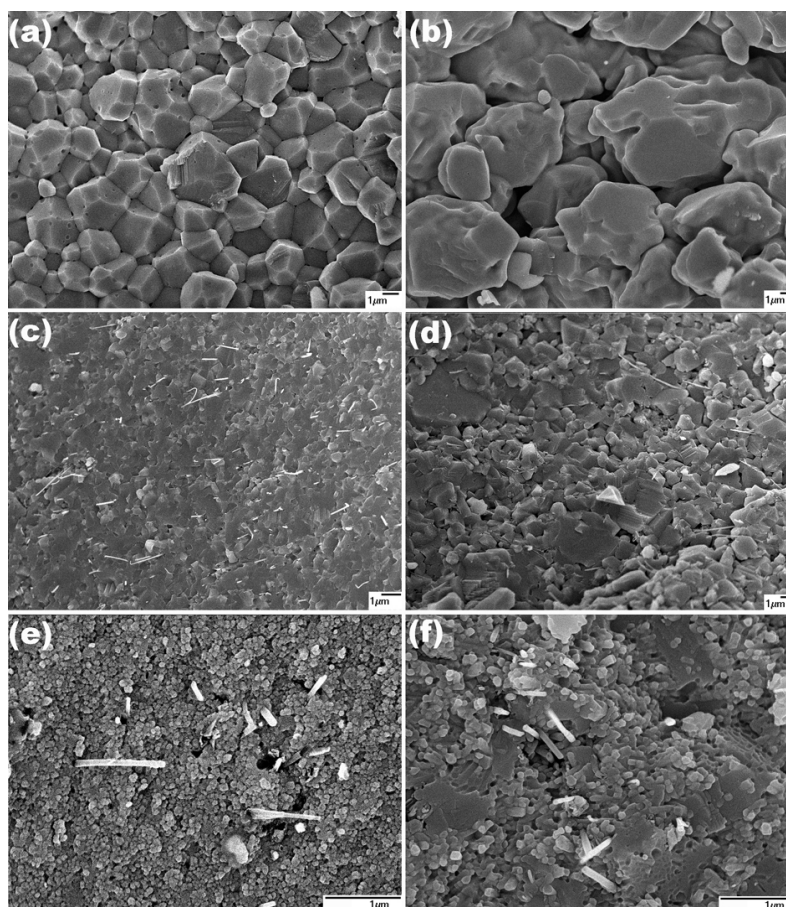


Figure 3. SEM images showing fracture surfaces of a pure alumina (a) before and (b) after SPD experiment, a 0.5 wt% BNNT/Al₂O₃ composite (c) before and (d) after SPD experiment, and a BNNT/Si₃N₄ composite (e) before and (f) after SPD experiment. SPD experiments were performed at 1450 °C for the Al₂O₃ based ceramics and at 1500 °C for the BNNT/Si₃N₄ composite. The constant strain rate is 10⁻⁴ s⁻¹. All scale bars are 1 μm.

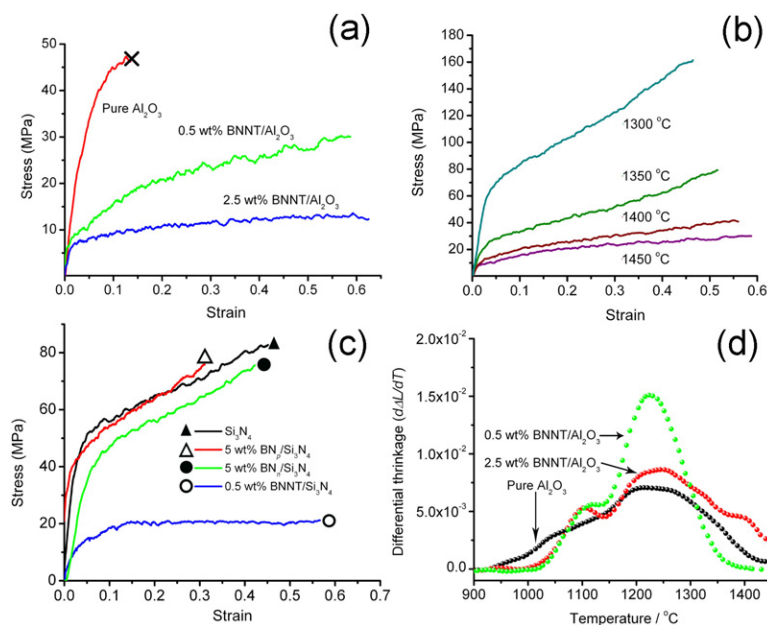


Figure 4. (a) Stress–strain curves of pure alumina and BNNT composites at 1450 °C; (b) stress–strain curves of 0.5 wt% BN_p/Al₂O₃ composites at different deformation temperatures; (c) stress–strain curves of Si₃N₄ composites doped with different BN materials at 1500 °C. All deformations were conducted at a constant strain rate of $1 \times 10^{-4} \text{ s}^{-1}$. (d) Differential temperature-dependent shrinkage curves of Al₂O₃ based ceramics with and without addition of BNNTs.

0.5 wt% BNNT/Al₂O₃ composite, the dynamic grain growth during deformation is also markedly suppressed accompanied with minimized cavitation (figure 3(d)). Therefore, the accommodation length evolution was favorably slow to match the SPD processes, such as grain rotation, grain boundary sliding and grain boundary diffusion. Although there abnormally grown alumina grains are still present, as reflected by the strain-hardening phenomenon (stress increases along with strain) and displayed by the strain–stress curve (figure 4(a)), surrounding small grains would act as fluidic balls that can promote the accommodation of cavities formed by the large grains sliding or rotating. The 2.5 wt% BNNT/Al₂O₃ composite exhibits a similar low true stress (7.1 MPa) at 1450 °C (figure 4(a)), but the strain-hardening phenomenon is largely alleviated.

Hexagonal BN powders (BN_p) are engineering lubricants utilized in machinable ceramics due to the weak van der Waals forces between layers [21]. The role of the interlayer-sliding mechanism, to the best of our knowledge, was never applied to address the SPD behavior. This may be due to the high sintering temperature needed for dense BN composites. In fact, the 2.5 wt% BN_p/Al₂O₃ composite could not be fully densified even at a sintering temperature up to 1700 °C at which the alumina grains grew rapidly (to more than 10 μm in diameter) which in practice deterred the plastic deformation. In order to understand the effect of BNNTs on SPD, the grain size of the ceramic matrix should be fixed. Therefore, three kinds of BN materials with different morphology and size, including BNNTs, micro-sized BN_p powders and nano-sized BN powders (BN_n, fabricated via high-energy milling method; average particle size ~ 80 nm), were incorporated into nanocrystalline Si₃N₄ ceramics whose grain size was maintained to be less than 100 nm in the resultant composites.

The average initial Si₃N₄ particle size is 70 nm. Obviously, the high-temperature strain–stress measurements show that neither BN_p/Si₃N₄ composite nor BN_n/Si₃N₄ composite benefit the superplasticity property when compared to SPD behavior of pure nanocrystalline Si₃N₄ ceramic, in spite of the high loading rate of 5 wt% (figure 4(c)). On the contrary, the 0.5 wt% BNNT/Si₃N₄ composite deforms plastically much easily and exhibits a true stress of lower than 20 MPa, which further enhances the SPD behavior of Si₃N₄ ceramics that has recently been achieved in nanocrystalline ceramics [16]. A scanning electron microscopy (SEM) image of deformed 0.5 wt% BNNT/Si₃N₄ composite depicts that although a few grains experienced abnormal growth during the deformation they are still immersed in a pool of nanosized equiaxed Si₃N₄ grains (figure 3(f)), which is distinct from the deformed pure nanocrystalline Si₃N₄ ceramic composed of elongated Si₃N₄ grains [17]. Nanosized equiaxed grains have very short accommodation lengths and are competent for filling the cavities formed by the movement of dynamically grown grains, which is similar to the case of BNNT/Al₂O₃ composites. From the ϵ – σ relationship, we obtained the stress exponent n to be definitely 1 which indicates that the main SPD mechanism is diffusion-controlled as in a pure nanocrystalline Si₃N₄. However, the calculated activation energy Q of $384 \pm 71 \text{ kJ mol}^{-1}$ is much lower than that of Si₃N₄ ($571.8 \text{ kJ mol}^{-1}$), indicating better deformation ability.

All the above experimental results indicate that the impact of BNNTs on superplasticity is evident. Although a carbon nanotube has been shown to be superplastically deformed at a bias voltage [10], BNNT was not observed to extend but was peeled off in our experiments, as shown in figure 4. Actually, the temperature used during the SPD tests was much lower than 2000 °C above which the defects

and constitutive elements (i.e. C in CNTs) become activated. Therefore, the intrinsic ductility of BNNTs at high temperature is not a factor at the current SPD conditions and should be excluded to account for the SPD enhancement. The microstructure variations and interactions between the BNNTs and matrix thus played an important role in the deformation behavior. First, the underlying attribution of BNNTs to superplasticity is due to their role in the suppression of static grain growth during a sintering stage, as displayed by the BNNT/ Al_2O_3 composite (figure 3(c)). This effect is owing to evenly distributed BNNTs located on the GBs of ceramics that effectively obstruct the mass transport between adjacent ceramic grains. For example, 0.5 wt% BNNTs (specific surface area is $40 \text{ m}^2 \text{ g}^{-1}$) would take $\sim 16\%$ GB area of alumina ceramic with an average grain size of 600 nm. Therefore, the GB diffusion and abnormal-grain-growth (Ostwald ripening mechanism) during the sintering process were, to a large extent, suppressed. Moreover, the sintering kinetic data verify that additional grain-rearrangement takes place in the BNNT/ Al_2O_3 composites, as disclosed in the temperature-dependent differential shrinkage curves (figure 4(d)). This grain-rearrangement occurs near 1100°C at which a liquid phase triggered by a high-frequency spark plasma might form on a Al_2O_3 grain surface when the reaction of alumina with BNNTs is thermodynamically unfavorable [14]. Zhan *et al* also pointed out that the spark plasma effect played a major role in the initial sintering process and promoted densification [7a]. Thus it is proposed that this rearrangement stage should correspond to rotation and sliding of surface-activated alumina grains on the outermost walls of BNNTs. Without BNNTs, the direct contact or squeezing of surface-activated alumina grains would promote the GB mass diffusion and lead to fast grain growth, as observed in pure alumina ceramics (figure 3(a)). Secondly, the embedded BNNTs in the composites could dissipate the concentrated stresses during the superplastic deformation, which would further inhibit the dynamic grain growth when composites are under compressive stress at high temperature. Otherwise, the high stress concentration at the ceramic GBs or corners will drive a rapid dissolution–precipitation process and accordingly result in grain-coarsening as in the deformed blank ceramic (figure 3(b)). It is a distinct function of a 1D tubular fiber that it can transfer and disperse the concentrated stress along the axial orientation [22]. Strong bonding between the BNNTs and matrix grains help the effective load transfer (figure 4(a)). It is imaginable that when one grain slides or rotates relative to another adjacent grain during deformation, the sandwiched BNNT will feel a shear stress in addition to a compressive stress. Strained BNNTs will transfer and disperse the stress along the axial orientation instead of normal to the grain surface. On the contrary, flake-like BN powders (whether their sizes are nanometers or micrometers) only pass stress between two ceramic grains without relaxation and thus have no effect on the dispersion of the accumulated stresses. Thirdly, a BNNT would be an efficient absorber of strain energy accumulated during the deformation. Distorted (bent, tense and twisted) BNNT layers during the deformation would be broken down and expose the inner BNNT shells when the stress is over the threshold strength. Although the *in situ* observation of this process is infeasible, some hints could be traced in the

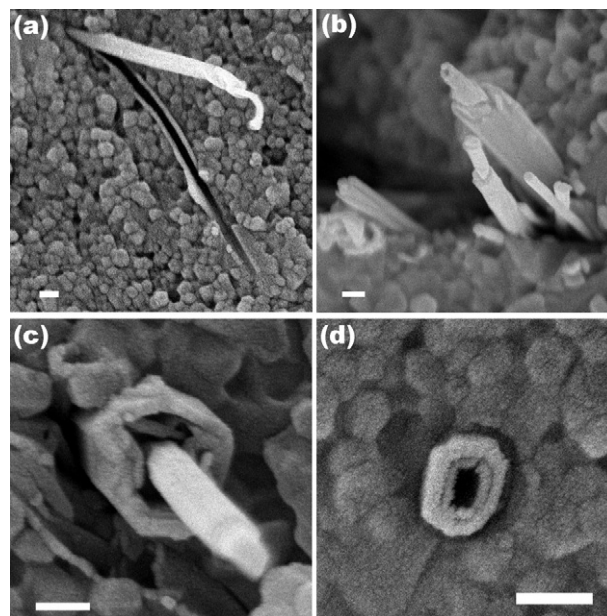


Figure 5. SEM images showing: (a) the outside wall of a BNNT sticking on Si_3N_4 grains and free-standing inner BNNT, (b) ‘sword-in-sheath’ structures of protruding BNNTs, (c) a protruding BNNT with distorted outside walls and (d) a compressed BNNT with a rectangle-like cross section. All scale bars are 100 nm.

fracture surface of deformed composites (figure 5). Most of BNNTs are vividly in ‘sword in sheath’ structures peculiar to the strong bonding of BNNTs’ outside walls with a ceramic matrix (figures 5(b) and (c)). These unsheathed structures simultaneously indicate that the compressive or shear load was incipiently taken mainly by the external walls and stepwisely transferred outside-in to the inner walls after the outer walls had been broken down under extreme stress. When another grain surface approaches these fresh inner walls of BNNTs, the whole peeling process would repeat as the stress accumulates to some extent. Obviously, the original round BNNT cross-section is always distorted to a nearly rectangular shape under compression (figure 5(d)). This distortion or peeling of BNNTs during the SPD process would convert much of the work to strain energy or apply it to break a B–N covalent bond, and leave little energy to the matrix for the formation of fresh surfaces (crack formation or propagation). This energy-absorption mechanism has been discussed to explain the contact-damage-resistant feature of CNT composites [23], and also was proposed to be principally responsible for the enhanced superplasticity of a ZrO_2 -spinel- Al_2O_3 composite in which plastic deformation of ZrO_2 acted as a stress-relaxant [8].

Finally we note that additional detailed studies of novel BNNT composite properties, for example fracture strength and thermal conductivity, are under way.

4. Conclusion

In summary, the present results show that a small addition of BNNTs (especially 0.5 wt%) will make typical engineering ceramics, such as Al_2O_3 and Si_3N_4 , readily much more moldable at a high temperature while their other characteristic

properties are not altered. In contrast, BN micro- or nano-sized powders were found not to be beneficial to the superplastic deformation behavior. The underlying SPD-enhancement mechanism is discussed in terms of the inhibition of static and dynamic grain growth of the matrix and energy-absorption mechanism of BNNTs. The unraveled capability of BNNTs to enhance the SPD behavior will make BNNTs promising components in cost-effective complex ceramics with good comprehensive mechanical properties.

References

- [1] Dresselhaus M S, Dresselhaus G and Eklund P C 1996 *Science of Fullerenes and Carbon Nanotubes* (San Diego, CA: Academic)
- Zhan G D, Kuntz J D, Wan J L and Mukherjee A K 2003 *Nat. Mater.* **2** 38
- Veedu V P, Cao A Y, Li X S, Ma K G, Soldano C, Kar S, Ajayan P M and Ghasemi-Nejhad M N 2006 *Nat. Mater.* **6** 457
- [2] Chopra N G and Zettl A 1998 *Solid State Commun.* **105** 297
- Suryavanshi A P, Yu M F, Wen J G, Tang C C and Bando Y 2004 *Appl. Phys. Lett.* **84** 2527
- Chang C W, Han W Q and Zettl A 2005 *Appl. Phys. Lett.* **86** 173102
- [3] Bansal N P, Hurst J B and Choi S R 2006 *J. Am. Ceram. Soc.* **89** 388
- [4] Daraktchiev M, Van de Moortele B, Schaller R, Coureau E and Forro U 2005 *Adv. Mater.* **17** 88
- [5] Wakai F, Sakaguchi S and Matsuno Y 1986 *Adv. Ceram. Mater.* **1** 259
- [6] Chokshi A H, Mukherjee A K and Langdon T G 1993 *Mater. Sci. Eng. R* **10** 237
- Chen I W and Xue L A 1990 *J. Am. Ceram. Soc.* **73** 2585
- [7a] Zhan G D, Garay J E and Mukherjee A K 2005 *Nano Lett.* **5** 2593
- [7b] Shen Z J, Peng H and Nygren M 2003 *Adv. Mater.* **15** 1006
- [7c] Chokshi A H, Mukherjee A K and Langdon T G 1993 *Mater. Sci. Eng. R* **10** 237
- [8] Kim B N, Hiraga K, Morita K and Sakka Y 2001 *Nature* **413** 288
- [9] Cha S I, Kim K T, Arshad S N, Mo C B and Hong S H 2005 *Adv. Mater.* **17** 1377
- [10] Huang J Y, Chen S, Wang Z Q, Kempa K, Wang Y M, Jo S H, Chen G, Dresselhaus M S and Ren Z F 2006 *Nature* **439** 281
- [11] Zhi C Y, Bando Y, Tang C C and Golberg D 2005 *Solid State Commun.* **135** 67
- [12] Xu X, Nishimura T, Hirosaki N, Xie R J, Zhu Y C and Yamamoto Y 2005 *J. Am. Ceram. Soc.* **88** 934
- [13] Celik-Aktas A, Zuo J M, Stubbins J F, Tang C C and Bando Y 2005 *Acta Crystallogr. A* **61** 533
- [14] Zhang G J, Yang J F, Ando M, Ohji T and Kanzaki S 2004 *Acta Mater.* **52** 1823
- [15] Flahaut E, Peigney A, Laurent C, Marliere C, Chastel F and Rousset A 2000 *Acta Mater.* **48** 380
- Huang Q, Gao L, Liu Y Q and Sun J 2005 *J. Chem. Mater.* **15** 1995
- [16] Srivastava D, Wei C Y and Cho K 2003 *Appl. Mech. Rev.* **56** 215
- Shi D L, Feng X Q, Huang Y G, Hwang K C and Gao H J 2004 *J. Eng. Mater. Technol.* **126** 250
- [17] Xu X, Nishimura T, Hirosaki N, Xie R J, Yamamoto Y and Tanaka H 2006 *Acta Mater.* **54** 255
- [18] Xue L A, Wu X and Chen I W 1991 *J. Am. Ceram. Soc.* **74** 842
- [19] Xue L A and Chen I W 1996 *J. Am. Ceram. Soc.* **79** 233
- [20] Tai Q and Mocellin A 1999 *Ceram. Int.* **25** 395
- [21] Kusunose T, Sekino T, Choa Y H and Niihara K 2002 *J. Am. Ceram. Soc.* **85** 2689
- [22] Qian D, Dickey E C, Andrews R and Rantell T 2000 *Appl. Phys. Lett.* **76** 2868
- [23] Wang X T, Padture N P and Tanaka H 2004 *Nat. Mater.* **3** 539